Ion-Pair and Solvent Relaxation Processes in Aqueous Na_2SO_4 Solutions

Richard Buchner,*,† Stephen G. Capewell, Glenn Hefter,* and Peter M. May

Chemistry Department, Division of Science, Murdoch University, Murdoch, W.A. 6150, Australia

Received: September 14, 1998; In Final Form: December 2, 1998

The complex dielectric permittivity of aqueous sodium sulfate solutions ($0.025 \leq c/\text{mol dm}^{-3} \leq 1.6$) has been determined in the frequency range $0.2 \leq \nu/\text{GHz} \leq 20$ with a commercial dielectric measurement system based on a vector network analyzer. The spectra were supplemented with interpolated literature data at $12 \leq \nu/\text{GHz} \leq 89$. To fit the complex permittivity spectra, a superposition of three Debye relaxation processes was necessary. The slow and intermediate dispersion steps are assigned to the tumbling motion of doubly solvent-separated (2SIP) and solvent-shared (SSIP) $NaSO_4^-$ ion pairs, respectively. The fast process, of amplitude S_3, is due to the collective relaxation of the solvent. Effective solvation numbers were deduced from the effect of Na_2SO_4 concentration on S_3. From the ion-pair dispersion amplitudes, S_1 and S_2, the concentrations c_{2SIP} and c_{SSIP}, and thus the overall stoichiometric stability constant, $\beta_{NaSO_4^-}$, were determined.

1. Introduction

The association of sodium and sulfate ions in concentrated aqueous solutions

$$Na_{aq}^{+} + [SO_4^{2-}]_{aq} \rightleftharpoons [NaSO_4]_{aq}^{-} \quad (1)$$

is of great importance in a variety of chemical systems of oceanographic,[1] geochemical,[2,3] and industrial[4] interest. Not surprisingly, a significant body of thermodynamic data has been accumulated on this equilibrium.[5−8] However, due to the weakness of the interaction of Na^+(aq) with SO_4^{2-}(aq) ions, the equilibrium constant is rather poorly characterized. Thus at 25 °C, the literature values of the standard equilibrium constant

$$K_A = \frac{\beta}{\text{dm}^3\,\text{mol}^{-1}} \frac{y_{IP}}{y_+ y_-} \quad (2)$$

where y_{IP} is the activity coefficient of the ion pair at concentration c_{IP} and y_+ and y_- are the activity coefficients of the free Na^+ and SO_4^{2-} ions at concentrations c_+ and c_-, respectively, range from 4.5 to 12.6 (see ref 8 for an overview). Disagreement among the various reported values for the ionic-strength (I) dependent stability constant β,

$$\beta = \frac{c_{IP}}{c_+ c_-} \quad (3)$$

is even larger.[8]

As both Na^+ and SO_4^{2-} are strongly solvated in water, their association should follow the three-step association mechanism of Eigen and Tamm[9] where 2SIP, SSIP, and CIP are respectively the doubly solvent-separated, solvent-separated, and contact ion pairs

$$Na_{aq}^{+} + [SO_4^{2-}]_{aq} \overset{\beta_{12}}{\rightleftharpoons} \underset{2SIP}{[Na^+\cdot OH_2\cdot OH_2\cdot SO_4^{2-}]_{aq}^{-}} \overset{\beta_{23}}{\rightleftharpoons} \underset{SSIP}{[Na^+\cdot OH_2\cdot SO_4^{2-}]_{aq}^{-}} \overset{\beta_{34}}{\rightleftharpoons} \underset{CIP}{[Na^+\cdot SO_4^{2-}]aq^{-}} \quad (4)$$

From eq 4 it can be seen that the stability constants of the individual reaction steps

$$\beta_{12} = \frac{c_{2SIP}}{c_+ c_-}; \qquad \beta_{23} = \frac{c_{SSIP}}{c_{2SIP}}; \qquad \beta_{34} = \frac{c_{CIP}}{c_{SSIP}} \quad (5)$$

relate to the overall stability constant β via

$$\beta = \beta_{12} + \beta_{12}\beta_{23} + \beta_{12}\beta_{23}\beta_{34} \quad (6)$$

with the total ion-pair concentration $c_{IP} = c_{2SIP} + c_{SSIP} + c_{CIP}$.

Ultrasonic relaxation data suggest a that a two-step association mechanism is sufficient to describe the equilibrium (1).[10] However, little is known about the nature of the involved species. Raman[11−13] and infrared[14] spectroscopy indicate negligible contact ion-pair (CIP) formation for aqueous sodium sulfate. But it should be noted that the difference in the vibrational frequencies of unperturbed SO_4^{2-} (free anions, 2SIP, SSIP) and sulfate directly bound to Na^+ (CIP) may be too small for a deconvolution of the bands. Data from a previous dielectric relaxation study suggested a predominance of doubly solvent-separated ion pairs (2SIP) at low concentrations but could not rule out the solvent-shared species (SSIP).[15]

Dielectric relaxation spectroscopy (DRS), which determines the complex (dielectric) permittivity spectrum of the sample

$$\hat{\epsilon}(\nu) = \epsilon'(\nu) - i\epsilon''(\nu) \quad (7)$$

seems to be especially suited for the investigation of ion-pair formation due to its selectivity for species with a permanent dipole moment, μ.[16−20] In comparison with other spectroscopic techniques, the free ions do not produce an interfering contribution to the $\epsilon(\nu)$ spectrum. Also, the dielectric response increases with μ^2, *i.e.*, for ion pairs, essentially with the square of the

* To whom correspondence should be addressed.

† Permanent address: Institut für Physikalische und Theoretische Chemie, Universität Regensburg, D-93040 Regensburg, Germany. E-mail: Richard.Buchner@chemie.uni-regensburg.de.

10.1021/jp983706c CCC: $18.00
Published on Web 01/29/1999

TABLE 1: Concentration, c, Average Effective Conductivity, κ_e, Dielectric Relaxation Parameters ϵ_1, τ_1; ϵ_2, τ_2; ϵ_3, τ_3; ϵ_∞, of a 3D Fit, and Variance of the Fit, s^2, of Aqueous Na_2SO_4 Solutions at 25 °C[a]

c	κ_e	ϵ_1	τ_1	ϵ_2	τ_2	ϵ_3	τ_3	ϵ_∞	s^2
0						78.37	8.36	5.65	[b]
0.0250	0.478 ± 0.003	78.98	335			77.55	8.16	5.69	0.027
0.0501	0.886 ± 0.002	79.18	238	76.85	25.0*F*	76.70	8.13	5.80	0.026
0.1009	1.62 ± 0.01	78.83	157	75.57	25.0*F*	75.06	8.01	5.86	0.045
0.1502	2.256 ± 0.006	78.82	150	74.79	25.0*F*	73.36	7.96	5.93	0.067
0.2019	2.89 ± 0.02	78.37	136	73.90	25.0*F*	72.02	7.89	6.17	0.127
0.2503	3.424 ± 0.005	77.66	114	73.13	25.0*F*	70.62	7.83	5.98	0.049
0.3028	4.01 ± 0.03	77.42	115	72.57	25.0*F*	68.93	7.72	6.09	0.077
0.4028	4.96 ± 0.01	75.82	112	71.65	25.0*F*	65.13	7.45	6.23	0.051
0.4038	5.00 ± 0.01	75.92	102	71.47	25.0*F*	65.38	7.50	6.39	0.112
0.5035	5.87 ± 0.03	74.53	101	70.40	24.2	63.35	7.43	6.08	0.049
0.5047	5.90 ± 0.02	74.47	98.3	70.57	25.0*F*	62.17	7.30	6.63	0.107
0.6042	6.68 ± 0.02	73.10	99.9	69.47	23.5	60.01	7.23	6.28	0.065
		73.11	105	69.73	25.0*F*	60.57	7.28	6.32	0.065
0.6057	6.69 ± 0.01	73.42	98.8	69.50	25.0*F*	60.77	7.29	6.60	0.125
0.7049	7.45 ± 0.01	71.71	100	68.70	25.4	59.01	7.26	6.43	0.067
0.8017	8.12 ± 0.01	69.87	100.0*F*[c]	68.15	27.0	57.29	7.23	6.28	0.072
0.8056	8.14 ± 0.01	70.36	112	68.08	26.7	57.47	7.21	6.52	0.084
0.9063	8.72 ± 0.05	68.73	98.5	66.60	24.8	54.14	7.03	6.70	0.114
1.0011	9.31 ± 0.03	67.07	100.0*F*	66.49	26.3	52.95	7.00	6.69	0.127
1.0057	9.34 ± 0.02	66.85	100.0*F*	66.15	25.5	52.18	6.98	6.78	0.074
1.1007	9.82 ± 0.03	66.09	100.0*F*	65.14	25.2	51.79	6.9*F*	6.08	0.121
1.2011	10.29 ± 0.02	64.10	100.0*F*	64.04	26.1	49.43	6.9*F*	6.93	0.076
1.4012	11.03 ± 0.03	61.65			25.9	47.03	6.8*F*	6.31	0.086
1.6034	11.58 ± 0.01	58.91			24.9	43.85	6.7*F*	6.08	0.082

[a] Units: c in mol dm^{-3}, κ_e in Ω^{-1} m^{-1}, τ_i in 10^{-12} s. [b] Data from ref 25. [c] F preset parameter (not adjusted).

charge separation. Thus, the sensitivity of DRS grows in the sequence CIP → SSIP → 2SIP, whereas other spectroscopic methods generally only monitor CIP and potentiometry detects only the overall level of association.

However, there are drawbacks of DRS that have hampered the interpretation of previous investigations[15,21,22] on weakly associating electrolytes ($K_A < 10$). Thus, although the frequency-dependent (relative) dielectric permittivity, $\epsilon'(\nu)$, the so-called dispersion curve, is directly accessible, the complementary dielectric loss $\epsilon''(\nu)$ is not. This is because the experimentally accessible total loss, $\eta''(\nu)$, includes not only $\epsilon''(\nu)$ but also an Ohmic loss term, $\eta''_\kappa(\nu)$, arising from the electric conductivity, κ, of the sample[23]

$$\eta''(\nu) = \epsilon''(\nu) + \eta''_\kappa(\nu) = \epsilon''(\nu) + \kappa/(2\pi\nu\epsilon_0) \qquad (8)$$

The κ contribution dominates at low frequencies and thus defines the minimum frequency, ν_{min}, to which ϵ'' (and also ϵ') can be determined with sufficient accuracy.[18] Since ion-pair relaxation times are typically 50−500 ps and the dispersion amplitudes (relaxation strengths) of weakly associated electrolytes are small compared to the solvent contribution, ν_{min} should be ideally <0.7 GHz for meaningful deconvolution. Only recently has instrumentation of sufficient accuracy become available to meet these requirements.[18,24]

In a previous publication[25] it was shown that a commercial dielectric measurement system based on a vector network analyzer could be used for the investigation of concentrated NaCl solutions provided a judicious calibration and measurement protocol was followed. Accordingly, because of the general interest in aqueous Na_2SO_4 [1−5] and its specific relevance to the study of the speciation in industrially-important concentrated aluminate solutions[8,26] where sulfate is often a major contaminant, a thorough DRS investigation of the Na_2SO_4/H_2O system was undertaken. This system is also a useful starting point for a systematic investigation of weak ion association in aqueous electrolytes because of the availability of the appropriate reference data.[15,21,27]

2. Experimental Section

Samples (100 mL) in the concentration range $0.025 \le c$/mol dm^{-3} ≤ 1.603 were prepared in volumetric flasks (0.1% accuracy) from analytical grade Na_2SO_4 (Ajax Chemicals, Australia) and Millipore (Milli-Q System) water. Dielectric measurements were performed at 25.0 ± 0.1 °C (temperature stability ±0.01 °C) with a Hewlett-Packard model HP 85070M dielectric probe system in the arrangement described in ref 25. For each series of measurements, usually comprising four to six samples, the VNA was calibrated with three standards—air, mercury, and Millipore water—thermostated to the measurement temperature. The calibration parameters for water (static permittivity $\epsilon = 78.37$, relaxation time $\tau = 8.26$ ps, Cole−Cole relaxation-time distribution parameter $\alpha = 0$, infinte frequency permittivity $\epsilon_\infty = 5.87$), which are optimized for the bandshape of its $\hat{\epsilon}(\nu)$ spectrum in the frequency range of the VNA, were taken from ref 25. Each solution was measured at least twice in different measurement series. $\epsilon'(\nu)$ and $\eta''(\nu)$ were generally recorded at 101 frequencies equidistant on a logarithmic scale between ν_{min} and $\nu_{max} = 20.05$ GHz. The value of ν_{min} was adapted to the conductivity of the sample: $0.2 \le \nu_{min}$/GHz ≤ 0.6.

For each spectrum the total loss of the sample, $\eta''(\nu)$, was corrected individually for the conductivity contribution, $\eta''_\kappa(\nu) = \kappa_e/(2\pi\nu\epsilon_0)$, where the effective conductivity, κ_e, was treated as an adjustable parameter. Table 1 lists the average values of κ_e obtained and their maximum scatter. The concentration dependence of the effective conductivity is given by a Casteel−Amis type equation[28]

$$\kappa_e = \kappa_{max}\left(\frac{c}{\mu_c}\right)^a \exp[-a(c/\mu_c - 1)] \qquad (9)$$

with the parameters $\kappa_{max} = 13.03 \pm 0.09$ Ω^{-1} m^{-1}, $\mu_c = 2.77 \pm 0.05$ mol dm^{-3}, and $a = 0.894 \pm 0.006$; $\sigma_{fit} = 0.03$ Ω^{-1} m^{-1}. These values are compared with the data obtained from conventional capillary cell measurements[21] in Figure 1. The

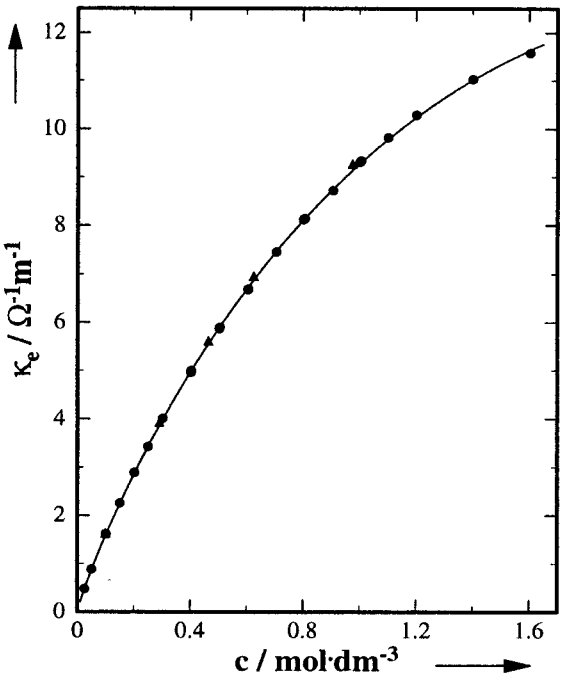

Figure 1. Average effective conductivity, κ_e (●), determined from the total loss spectrum, $\eta''(\nu)$, and conductivity data from ref 21 (▲). The solid line is calculated from the parameters of eq 9.

general trends are very similar, but κ_e is always smaller than the measured results by 1−2%. This suggests that the mathematical model for the probehead/sample interface is not fully adequate at high conductivities,[29] yielding values that are slightly too small for κ and hence for η''. However, from the following comparison with literature data it seems that neither $\epsilon'(\nu)$ nor $\epsilon''(\nu)$ are affected by this small systematic error.

For each sample, the $\hat{\epsilon}(\nu)$ spectra recorded in different measurement series were combined and, for $c \leq 1$ mol dm^{-3}, supplemented with the waveguide-interferometer data of Barthel et al.[21] (tabulated in the data collection[27]) at 12 GHz and at 27 $\leq \nu$/GHz $\leq$ 89. The latter were interpolated to the investigated concentrations by appropriate nonlinear functions. Data reported for the Ku-band region (12.4−18 GHz) were not included because of a systematic deviation of ϵ'' at high concentrations, which is obvious from the graphs of ref 27 and which has been discussed in ref 30.

Figure 2 shows that $\hat{\epsilon}(\nu)$ obtained with the VNA and the interpolated interferometer data match extremely well so that a combined analysis is possible. Also included in Figure 2 are the original data at the other frequencies of Barthel et al. at their lowest electrolyte concentration, $c = 0.099\ 43$ mol dm^{-3}, which is sufficiently close to allow a direct comparison with our $\hat{\epsilon}(\nu)$ at 0.1009 mol dm^{-3}. The good agreement over the entire frequency range, as well as the match of the VNA $\hat{\epsilon}(\nu)$ with the interpolated interferometer data up to the highest concentration of ref 21, suggests that within the conductivity and permittivity range covered by this investigation, ϵ' and ϵ'' can be determined with an accuracy of approximately ±1.5% relative to the static permittivity of the calibration standard (water).

3. Data Analysis and Results

The spectra were fitted to plausible relaxation models based on the superposition of up to four Havriliak−Negami equations or variants thereof, as described in ref 25. It turns out that for 0.1 $\leq c$/mol dm$^{-3} \leq$ 1.1 the superposition of three Debye

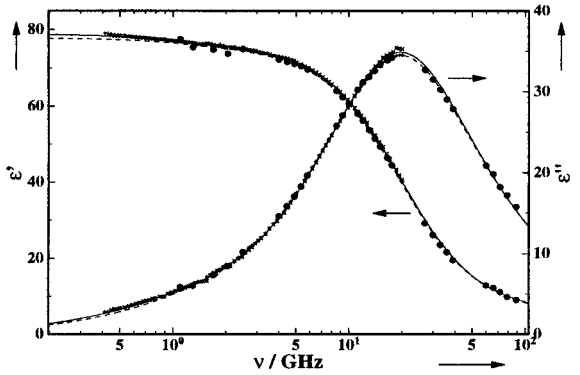

Figure 2. Dielectric dispersion, $\epsilon'(\nu)$, and loss spectrum, $\epsilon''(\nu)$, of a 0.1009 mol dm^{-3} Na_2SO_4 solution in water at 25 °C. Experimental data are obtained with the Murdoch VNA (×, + are results of two independent calibrations) and from the waveguide interferometers of Barthel et al.[21,27] (●, interpolated to 0.1009 mol dm^{-3} for $\nu = 12$ GHz and $\nu \geq 27$ GHz, original data at 0.099 43 mol dm^{-3} elsewhere). The solid line represents a superposition of three Debye relaxation processes fitted to the combined data. The broken line represents the three-Debye fit of Barthel et al. to their data at 0.099 43 mol dm^{-3}.

processes (the "3D model" hereafter)

$$\hat{\epsilon}(\nu) = \frac{\epsilon_1 - \epsilon_2}{1 + \mathrm{i}2\pi\nu\tau_1} + \frac{\epsilon_1 - \epsilon_3}{1 + \mathrm{i}2\pi\nu\tau_2} + \frac{\epsilon_3 - \epsilon_\infty}{1 + \mathrm{i}2\pi\nu\tau_3} + \epsilon_\infty \quad (10)$$

where $\epsilon = \epsilon_1$ is the "static" and ϵ_∞ the "infinite frequency" permittivity of the solution, yields the smallest variance, s^2. At $c = 0.025$ mol dm^{-3} the amplitude of the intermediate relaxation process, $S_2 = \epsilon_2 - \epsilon_3$, becomes too small to be detected ($\epsilon_2 \rightarrow \epsilon_3$) and above 1.2 mol dm^{-3} the amplitude of the low-frequency process, $S_1 = \epsilon_1 - \epsilon_2$, falls below the noise level ($\epsilon \rightarrow \epsilon_2$). However, from all considered relaxation models, 3D with vanishing S_2 at $c \rightarrow 0$ and $S_1 \rightarrow 0$ at high concentrations is the only model that yields a set of self-consistent parameters (limiting permittivities ϵ_1, ϵ_2, ϵ_3, ϵ_∞ and relaxation times $\tau_1 > \tau_2 > \tau_3$) for the individual dispersion steps. Only for the 3D model does the variation of the parameters remain smooth over the entire concentration range and can the relaxation processes be reasonably assigned (see section 4).

Unconstrained fits of the 3D model suggested that $\tau_2 \approx 25$ ps over the entire concentration range, whereas the relaxation time of the slow solute process flattened off to $\tau_1 \approx 100$ ps above 0.4 mol dm^{-3}. Therefore, τ_1 and τ_2 were preset to these values in the concentration ranges where the corresponding dispersion amplitudes, S_1 and S_2, were small, if this led to an improvement of the variance. At concentrations where no interferometer data were available, τ_3 was preset to the value extrapolated from the data at $c \leq 1$ mol dm^{-3} with

$$(\tau_3/\mathrm{ps})^{-1} = a_0 + a_1 \exp[-c/(\mathrm{mol\ dm^{-3}})] \quad (11)$$

where $a_0 = 0.1555 \pm 0.0007$ and $a_1 = -0.034 \pm 0.001$; $\sigma_{\mathrm{fit}} = 0.06$.

The fitting parameters and s^2 obtained with this procedure are summarized in Table 1. The repercussions of fixing one of the parameters on the results obtained for the other parameters are exemplified for $c = 0.6042$ mol dm^{-3}, where neither of the two parameter sets is favored as judged by their s^2 values. Within the concentration range of the experiments the permittivity parameters $\epsilon_i(c)$ ($\epsilon_i = \epsilon_1$, ϵ_2, ϵ_3, ϵ_∞) could be adequately described by the polynomial

TABLE 2: Coefficients a_j and Standard Deviations σ_{fit} of the Polynomial Eq 12, Valid for $0 \le c \le c_{max}$, for the Permittivity Parameters ϵ_1, ϵ_2, ϵ_3, and ϵ_∞ of Aqueous Na_2SO_4 Solutions at 25 °C[a]

ϵ_i	$\epsilon_i(0)$	a_1	a_2	a_3	a_4	σ_{fit}	c_{max}
ϵ_1	78.37F[b]	4.4 ± 0.3		−28.1 ± 0.9	12.5 ± 0.5	0.19	1.6
ϵ_2	78.37F	−1.1 ± 0.9	−35.3 ± 3.8	43.9 ± 4.7	−19.7 ± 1.9	0.15	1.6
ϵ_3	78.37F		−41.3 ± 0.8	15.8 ± 0.8		0.53	1.6
	78.37 ± 0.11		−32.1 ± 0.4			0.20	0.4
ϵ_∞	5.81 ± 0.05		0.91 ± 0.08			0.14	1.0

[a] Units: a_j in $dm^{3j/2}$ $mol^{-j/2}$, $j = 1-4$, c_{max} in mol dm^{-3}. [b] F preset parameter (not adjusted).

$$\epsilon_i(c) = \epsilon_i(0) + \sum_{j=1}^{4} a_j c^{j/2} \tag{12}$$

The coefficients and the standard deviation of the fit, σ_{fit}, are collected in Table 2. From these data errors of $\sigma(S_1) \approx 0.4$ and $\sigma(S_2) \approx 0.7$ can be estimated for the amplitudes of the low- and the intermediate-frequency process, respectively.

Barthel et al. also used a 3D model to fit their $\hat{\epsilon}(\nu)$ over the frequency range $1.1 \le \nu/\text{GHz} \le 89$.[15,21] However, only the parameters of their process s1 and of our dispersion step 3, with relaxation times around 8 ps, can be directly compared. Both characterize the cooperative relaxation of the hydrogen-bond network of water. Because of their somewhat higher value of ν_{min}, 1.1 GHz, Barthel and co-workers were only able to resolve a single solute relaxation process at low frequencies (relaxation time τ_{IP}), whereas our analysis indicates two dispersion steps in this region with $\tau_2 < \tau_{IP} < \tau_1$. Both processes can be assigned to ion-pair species; *cf.* section 4. The fast solvent process claimed,[21] with $\tau_{s2} \approx 1.5$ ps, can be generally resolved in the combined spectra at $c \le 1$ mol dm^{-3} by using a 4D model. However, since we had to rely on the interpolated $\epsilon(\nu)$ data of Barthel et al. at $\nu > 20$ GHz and since s^2(4D) was usually not better than s^2(3D), at the cost of an increased scatter of all fitting parameters, this process was not considered further. It does not in any way significantly impact on the slower processes of interest here.

4. Discussion

4.1. Solute Relaxation. The magnitude of τ_1 is in the range typically found for solute relaxation processes[20] so that the assignment of the low-frequency dispersion step, designated by the index 1, to the tumbling motion of an ion-pair species is straightforward. From the magnitude and the concentration dependence of S_3 and τ_3 it is also obvious that the high-frequency process is due to the solvent. However, the origin of the intermediate dispersion step, characterized by S_2 and τ_2, is not immediately obvious. The value of τ_2 (≈25 ps) is considerably smaller than the ion-pair relaxation times (>80 ps) usually found for aqueous solutions. For aqueous tetraalkylammonium halides, an intermediate relaxation process with a similar time constant has been attributed to the solvent.[20,31] On the other hand Pottel, claims $\tau \approx 50$ ps for SSIP of transition metal sulfates[16] and $\tau_{IP} < 50$ ps is observed for a process that has been attributed to CIP in high concentrations of aqueous $CuCl_2$.[21]

A strong argument in favor of assigning process 2 to ion pairs is the concentration dependence of S_1. The assumption that only process 1 is due to ion pairs would imply negligible association at $c \ge 1$ mol dm^{-3} (*cf.* Figure 4), which is unlikely on the basis of recent potentiometric results[8] that show that ion association remains significant in high ionic strength background electrolytes. This is corroborated by a comparison of τ_2 with estimates of the rotational correlation time, τ', of model ion pairs at $c \to 0$, Table 3, obtained with the modified Stokes−Debye−Einstein equation[32]

TABLE 3: Major Semiprincipal Axis, a, Polarizability, α, Dipole Moment, μ, Molecular Volume, V, Shape Factor, $f_\perp$, and Rotational Correlation Times, τ', Predicted by Eq 13 for *Slip* and *Stick* Boundary Conditions of Rotational Diffusion, for the Model Ion Pairs CIP, SSIP, and 2SIP[a]

ion pair	a	α	μ	V	$f_\perp$	τ'_{slip}	τ'_{stick}
CIP	3.56	4.011	17.75	99	1.14	6	73
SSIP	4.99	5.455	36.62	139	1.46	29	132
2SIP	6.41	6.899	54.60	179	1.88	75	218

[a] Units: a in 10^{-10} m, α in 10^{-30} $4\pi\epsilon_0$ m^3, μ in 3.336×10^{-30} C m, V in 10^{-30} m^3, τ'_{slip} and τ'_{stick} in 10^{-12} s.

$$\tau' = \frac{3Vf_\perp C\eta}{k_B T} \tag{13}$$

In the calculation of τ' it is assumed that the ion-pair volume V can be approximated by a prolate ellipsoid of semiprincipal axes $a = r_+ + r_- + 2nr_s$ and $b = c = r_-$. $r_+ = 98$ pm, $r_- = 258$ pm, and $r_s = 142.5$ pm, which are the radii of Na^+, SO_4^{2-}, and H_2O, respectively;[15] n is the number of water molecules between the ions with $n = 0$ for CIP, $n = 1$ for SSIP, and $n = 2$ for 2SIP. The shape factor $f_\perp$ is defined in ref 32, $C = 1$ for *stick* boundary conditions of rotational diffusion and $C = 1 - f_\perp^{-2/3}$ applies for *slip* motion, and η is the viscosity of the solution. Since hydrodynamic boundary conditions are likely to be closer to slip for rotation on a molecular scale,[32,33] the results suggest CIP or SSIP as possible species for the intermedidate relaxation process. For the low-frequency dispersion step, 2SIP is likely but SSIP cannot be ruled out. Since $f_\perp$ is closer to unity, thus compensating for the increased V, the conclusion remains true even if the ion pairs rotate with a tightly bound solvation layer. From the above arguments it seems plausible to assign the observed relaxation processes 1 and 2 to two ion-pair species of reaction 4 and, according to the relaxation times, the combinations 2SIP/SSIP, SSIP/CIP, and 2SIP/CIP must be considered when attempting a quantitative analysis of the dispersion amplitudes S_1 and S_2.

For a dipole mixture with n independent relaxation processes i, the concentrations c_i of the relaxing species—of dipole moment μ_i and polarizability α_i—are related to the dispersion amplitudes S_i according to

$$c_i = \frac{3(\epsilon + (1-\epsilon)A_i)}{\epsilon} \frac{k_B T \epsilon_0}{N_A} \frac{(1-\alpha_i f_i)^2}{g_i \mu_i^2} S_i \tag{14}$$

In eq 14 ϵ_0 denotes the vacuum permittivity, k_B and N_A are respectively the Boltzmann and Avogadro constants, and T is the (Kelvin) temperature.[15,34] Similar to the g factor of the Kirkwood−Froehlich equation,[23] the empirical factor g_i accounts for dipole−dipole correlations between the dipoles i. The field factor f_i of the ellipsoidal reaction field is given by the expression

$$f_i = \frac{3}{4\pi\epsilon_0 a_i b_i^2} \frac{A_i(1-A_i)(\epsilon-1)}{\epsilon + (1-\epsilon)A_i} \tag{15}$$

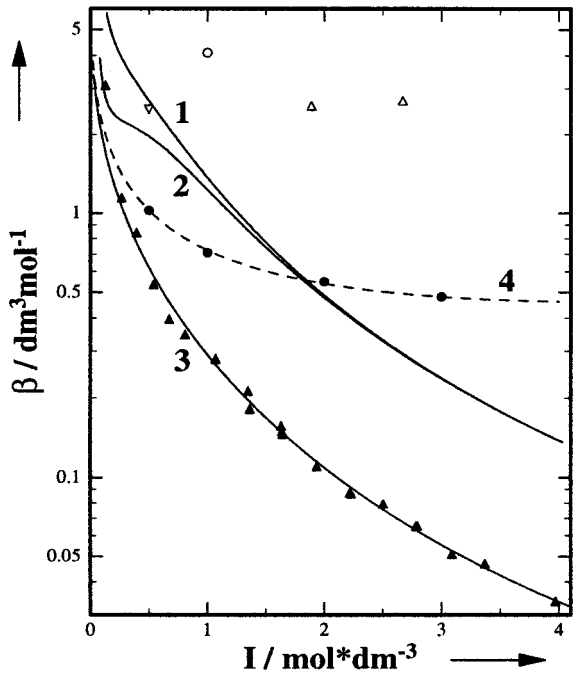

Figure 3. Overall stability constants, $\beta(NaSO_4^-(aq))$, in water at 25 °C as a function of ionic stength I. Curves 1−3 are obtained from the DRS data for the assignments of the relaxation processes 1 and 2 to the ion-pair species SSIP and CIP (curves 1), 2SIP and CIP (curve 2), and 2SIP and SSIP (curve 3), respectively. Curves 1 and 2 are calculated from the parameters of table 2, curve 3 represents the fit of the Guggenheim type equation (17) to the experimental data (▲). Also included are the β values obtained from potentiometric measurements in the presence of supporting electrolytes by Capewell et al.[8] (● and curve 4, CsCl), Luts et al.[40] (○, $NaClO_4$), Sapieszko et al.[41] (△, $(CH_3)_4NCl$), and Santos et al.[42] (▽, NaCl).

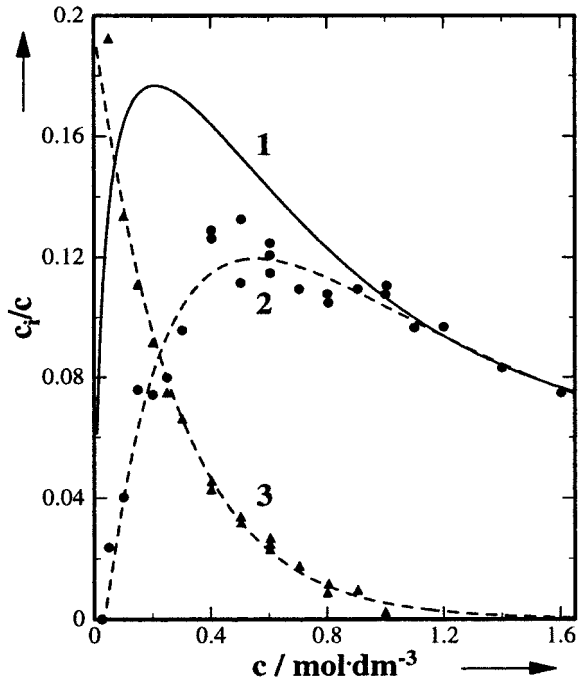

Figure 4. Relative concentrations, c_{IP}/c, of all ion pairs (curve 1), of SSIP (curve 2), and of 2SIP (curve 3) in aqueous Na_2SO_4 solutions at 25 °C. Data are calculated by assuming that the relaxation processes 1 and 2 are due to 2SIP and SSIP, respectively, using the parameters of eq 17 for curve 1 and the coefficients of Table 2 for curves 2 and 3.

where $A_i = {}^1/_3$ for a spherical reaction field and

$$A_i = -\frac{1}{p_i^2 - 1} + \frac{p_i}{(p_i^2 - 1)^{3/2}} \ln(p_i + \sqrt{p_i^2 - 1}) \quad (16)$$

for semiaxis ratios $p_i = a_i/b_i \neq 1$.[23]

Table 3 summarizes the input data of eqs 14−16 for the calculation of ion-pair concentrations from S_1 and S_2. The dipole moments given by Barthel et al.[15] for the center of hydrodynamic stress[33,35] as the pivot of ion-pair rotation were taken and for the polarizability $\alpha = \alpha(Na^+) + \alpha(SO_4^{2-}) + n\alpha(H_2O)$, with $n = 0, 1, 2$, was assumed by using the data of their Table 1. For ion pairs $g_i \approx 1$ can be assumed.

From S_1 and S_2, ion-pair concentrations c_i and stability constants β were calculated for the possible ion-pair combinations, IP1/IP2, of 2SIP/SSIP, SSIP/CIP, and 2SIP/CIP. Figure 3 summarizes the results obtained for β as a function of ionic strength. For the Na_2SO_4 solutions investigated, the ionic strength, defined as $I = (\sum z_j^2 c_j)/2$ with z_j and c_j as the charges and concentrations of all ionic species j, is calculated as $I = 3c - 2c_{IP}$. Although the dispersion amplitudes of the two most dilute solutions are reasonable within their error limits, $\sigma(S_1) \approx 0.4$ and $\sigma(S_2) \approx 0.7$, a close inspection of the data reveals that S_1 is systematically overestimated and S_2 is too small, leading to unacceptably large systematic errors for the relative concentrations c_i/c of all species; see curves 2 and 3 of Figure 4. Therefore, these were not considered in the determination of K_A.

In line with the activity coefficients predicted by the Debye-Hückel theory, all models exhibit a considerable decrease of β with increasing I but differ markedly in magnitude and concentration dependence. For the assignments SSIP/CIP (curve 1 of Figure 3) and 2SIP/SSIP (curve 3), β can be fitted with an extended Guggenheim-type semiempirical equation[36] with the additional adjustable parameter c_β for curve 3

$$\log \frac{\beta}{\mathrm{dm^3\ mol^{-1}}} = \log K_A - \frac{A|z_+z_-|\sqrt{I}}{1 + \sqrt{I}} + b_\beta I + c_\beta I^{3/2} \quad (17)$$

$A = 1.023\ \mathrm{dm^{3/2}\ mol^{-1/2}}$ for water at 25 °C. The model SSIP/CIP yields the parameters $K_A = 24.0 \pm 1.1$ and $b_\beta = -0.23 \pm 0.01\ \mathrm{dm^3\ mol^{-1}}$ with $\sigma_{fit} = 0.05$ (in this case an adjustable c_β did not improve the quality of the fit). For the model 2SIP/SSIP $K_A = 6.7 \pm 0.3$, $b_\beta = -0.44 \pm 0.03\ \mathrm{dm^3\ mol^{-1}}$ and $c_\beta = 0.10 \pm 0.02\ \mathrm{dm^{9/2}\ mol^{-3/2}}$ with $\sigma_{fit} = 0.03$ was obtained.

The most reliable literature data for the sodium sulfate standard association constant are probably that calculated by Reardon[37] from activity coefficients, $K_A = 6.6 \pm 0.8$, the potentiometric data of Pokrovski et al.,[3] $K_A = 5.8$, and that of Capewell et al.,[8] $K_A = 6.82 \pm 0.08$. An unlikely upper limit of 12.6 is given by the conductivity data of Fisher and Fox.[38] Obviously, the assignment of the slow relaxation process to SSIP and of the intermediate dispersion step to CIP is not compatible with these data. In contrast, the equilibrium constant derived for the combination 2SIP/SSIP is in good agreement with the literature data.

The model 2SIP/CIP (curve 2 of Figure 3) also yields a K_A value that is compatible with the literature data. However, the "hump" in β around $I = 0.5\ \mathrm{mol\ dm^{-3}}$, which prevents the application of eq 17, as well as the implied *direct* equilibrium between doubly solvent-separated and contact ion pairs is at variance with current theories on ion association.[39] It is also unlikely that the implied CIP fractions of $c_{CIP}/c > 0.3$ above $0.2\ \mathrm{mol\ dm^{-3}}$ would not be detected by vibrational or NMR spectroscopy. The tentative assignment of process 1 to an

unresolved superposition of 2SIP and SSIP dispersions (split into S_1^{2SIP} and S_1^{SSIP} by assuming a weighted geometric average of τ_1[31]) and of process 2 to CIP produces an even larger "hump" and hence can also be ruled out.

From the above discussion it may be concluded that in aqueous sodium sulfate solutions ion association predominantly leads to the formation of 2SIP and SSIP. Although the standard equilibrium constant is small ($K_A = 6.7$ is obtained from the present measurements), it is evident from the relative ion-pair concentrations shown in Figure 4 that the relative and absolute concentrations of ion pairs are far from negligible over the investigated concentration range. At $c \approx 0.2$ mol dm^{-3} almost 18% of the anions are bound to Na^+ with comparable amounts of 2SIP and CIP. At 1.6 mol dm^{-3} the total ion-pair fraction is still 7.5% (curve 1). 2SIP predominates at $c \leq 0.2$ mol dm^{-3} but becomes negligible above 1 mol dm^{-3} (curve 3; note that the line calculated from the parameters of Table 2 is not realistic for $c < 0.1$ mol dm^{-3}). SSIP amounts to about 12% of the total Na_2SO_4 concentration around 0.5 mol dm^{-3} and remains the dominating ion-pair species at high concentration.

Included in Figure 3 are results for β obtained from potentiometric measurements of dilute Na_2SO_4 solutions in the background electrolytes $NaClO_4$ (○),[40] NaCl (▽),[42] $(CH_3)_4NCl$ (△),[41] and CsCl (●, curve 4).[8] Although the differences between these investigations may reflect the differing quality of the data, all show a specific influence of the background electrolyte on the degree of sodium binding by SO_4^{2-}. For CsCl this may possibly be traced to weak $Cs^+\cdots SO_4^{2-}$ interactions.[8] More importantly, in all these studies $\beta \geq 0.5$ even at very high I, whereas in the concentrated Na_2SO_4 solutions of the present investigation β drops to 0.07 at the highest concentration (Figure 3, curve 3). This may arise from a weakening of the forces between individual $Na^+\cdots SO_4^{2-}$ pairs due to the presence of more competing ions of the same kind, *i.e.*, with equally strong interactions. Formally, this would correspond to increased activity coefficients y_+ and y_- compared to the studies with a more or less "inert" background electrolyte. Alternatively, the formation of nonpolar symmetric triple ions $Na^+\cdots SO_4^{2-}\cdots Na^+$, might be envisaged.

For a single-step equilibrium it can be shown that the ion-pair relaxation time τ_{IP} is given by

$$\tau_{IP}^{-1} = (\tau'_{IP})^{-1} + (\tau_{ch})^{-1} \tag{18}$$

In other words, the decay of the ion-pair contribution to the sample polarization occurs via two parallel pathways. These are characterized by the rotational correlation time of the ion-pair, τ'_{IP}, and the "chemical" relaxation time τ_{ch} determined by the rate constants of ion-pair formation, k_{12}, and decay, k_{21}, and explain the decrease of τ_{IP} with increasing c often observed for such equilibria.[43] An appropriate working equation that incorporates the viscosity dependence of τ'_{IP} with the help of eq 13 is

$$Y = V_e^{-1} + k_{12}X \tag{19}$$

with

$$Y = \frac{3}{k_B T}\frac{\eta}{\tau_1} \quad \text{and} \quad X = \frac{3\eta}{k_B T}(K_A^{-1} + 3c - 2c_{IP})$$

where $V_e = Vf_\perp C$ is the effective volume of the ion pair.[15] Equation 19 should be valid for τ_1 provided the formation of SSIP is slow compared to equilibration between the free ions and 2SIP.

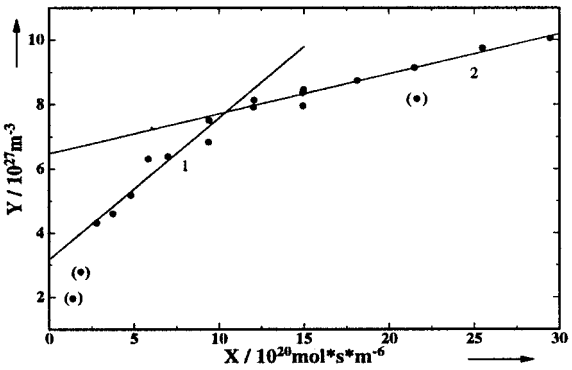

Figure 5. Analysis of τ_1 with eq 19. Curve 1 yields $V_{eff} = (316 \pm 38) \times 10^{-30}$ m^3 $k_{12} = (4.4 \pm 0.6) \times 10^9$ dm^3 mol^{-1} s^{-1}, curve 2 gives V_{eff} $(154 \pm 4) \times 10^{-30}$ m^3 and $k_{12} = (1.24 \pm 0.10) \times 10^9$ dm^3 mol^{-1} s^{-1}. Bracketed points are not included in the fits.

The rotational correlation time rises from $\tau'_{2SIP}(0) \approx 75$ ps, Table 3, to roughly 150 ps in the investigated concentration range due to the viscosity increase, whereas the chemical relaxation times determined by Gilligan and Atkinson[10] increase from 500 ps at 0.3 mol dm^{-3} to 720 ps at 1 mol dm^{-3}. The experimental relaxation rate, $1/\tau_1$, is therefore dominated by ion-pair rotation, but a chemical contribution should be detectable. Figure 5 illustrates the application of eq 19 to the 2SIP relaxation time τ_1 with the viscosity data taken from refs 44−46. Two linear branches may be defined corresponding to the parameters V_e and k_{12} given in the figure caption. However, the data do not follow a single straight line. In line with Gilligan and Atkinson,[10] who conclude that alkali metal association with sulfate proceeds by the almost diffusion-controlled formation of an outer-sphere complex followed by rapid conversion to an (unspecified) inner-sphere complex, this indicates that the time scales for the formation of 2SIP and SSIP are not sufficiently separated to use eq 19 for a reliable determination of the rate constants k_{12} and $k_{21} = k_{12}/K_A$ from τ_1.

4.2. Solvent Relaxation. The dispersion amplitude of the solvent, $S_3(c) = \epsilon_3(c) - \epsilon_\infty(c)$, exhibits a considerable decrease with increasing electrolyte concentration, c, which suggests extensive ion−solvent interactions,[19,20] as expected. Following the route outlined in ref 25, but starting from eq 14 with $A_3 = {}^1/_3$ due to the presence of the ion-pair relaxation processes and using a constant f_3, we calculated the apparent water concentration, c_s^{ap}, in the solution from $S_3(c)$ using

$$c_s^{ap}(c) = \frac{g_3(c)}{g_3(0)}c_s^{bulk} = c_s(0)F_{Cav}\frac{2\epsilon(c)+1}{\epsilon(c)}S_3^{eq}(c) \tag{20}$$

with

$$F_{Cav} = \frac{\epsilon(0)}{S_3(0)[2\epsilon(0)+1]}$$

Note that the concentration of undisturbed bulk water, c_s^{bulk}, is not directly accessible due to a possible change of the dipole correlation factor g_3 with c. Moreover, with respect to the solvent it cannot simply be assumed that $g_3 \approx 1$.

The equilibrium amplitude of the solvent dispersion, S_3^{eq}, is given by

$$S_3^{eq}(c) = S_3(c) + \Delta_{kd}\epsilon(c) \tag{21}$$

For the contribution due to kinetic depolarization, $\Delta_{kd}\epsilon$, the prediction of the Hubbard−Onsager continuum theory[47,48] for

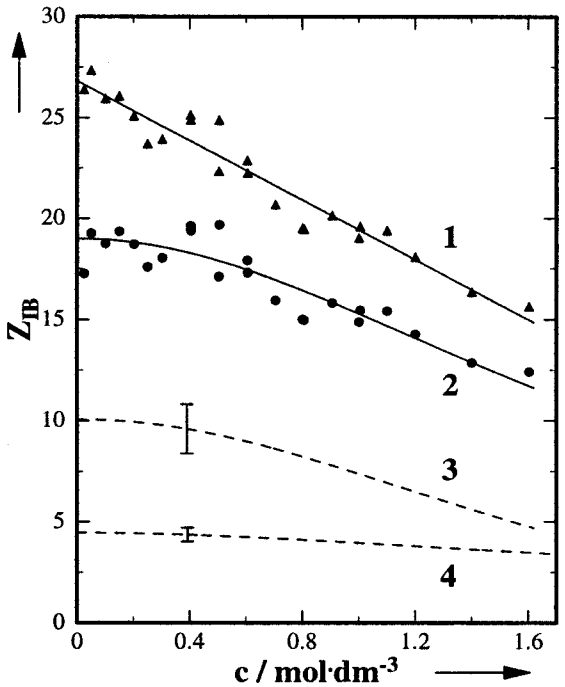

Figure 6. Effective solvation numbers of Na_2SO_4 at 25 °C assuming negligible kinetic depolarization ($\xi = 0$, curve 1) and kinetic depolarization under slip boundary conditions ($\xi = \xi_{slip}$, curve 2). Curve 3 is the effective solvation number of sulfate, $Z_{IB}^{slip}(SO_4^-)$, calculated from curve 2 and $Z_{IB}^{slip}(Na^+) = Z_{IB}^{slip}(NaCl)$, curve 4.[25]

slip boundary conditions ($p = {}^2/_3$) for the motion of the, eventually solvated, ions

$$\Delta_{kd}\epsilon(c) = \xi\kappa(c); \qquad \xi = p\frac{\epsilon(0) - \epsilon_\infty(c)}{\epsilon(0)}\frac{\tau(0)}{\epsilon_0} \quad (22)$$

as well as $\Delta_{kd}\epsilon = 0$, and hence $\xi = 0$, were considered. Although physically reasonable values of c_s^{ap} can be obtained for Na_2SO_4 solutions with the stick limit ($p = 1$) of eq 22, they will not be discussed since our NaCl results[25] for such boundary conditions imply a negative solvation number for Na^+.

Comparison of c_s^{ap} with the analytical water concentration, c_s, of the solutions yields the effective solvation number Z_{IB}

$$Z_{IB} = (c_s - c_s^{ap})/c \quad (23)$$

with curve 1 of Figure 6 obtained by assuming negligible kinetic depolarization, $\xi = 0$, and curve 2 for kinetic depolarization with slip boundary conditions, $\xi = \xi_{slip}$. Whereas $Z_{IB}^{\xi=0}$ decreases linearly, with intercept $Z_{IB}^{\xi=0}(0) = 26.8 \pm 0.3$ and slope -7.4 ± 0.4 dm^3 mol^{-1} ($\sigma_{fit} = 0.9$), the slip results are best fitted by $Z_{IB}^{slip}(c) = 1/(a_o + a_1c^2)$ with $a_o = 0.0526 \pm 0.0008$ and $a_1 = 0.0127 \pm 0.0014$ dm^6 mol^{-2} ($\sigma_{fit} = 0.9$), which yields the zero-concentration intercept $Z_{IB}^{slip}(0) = 19.0 \pm 0.3$. Due to the wider frequency range of the present combined spectra and the resulting change of the relaxation model, the present values of $Z_{IB}^{\xi=0}(0)$ and $Z_{IB}^{slip}(0)$ are significantly larger than the corresponding results of 21.2 and 13.6 of Barthel et al.[21]

In ref 25 it was argued that kinetic depolarization with slip boundary conditions applies to aqueous NaCl. For the chloride ion the data suggest $Z_{IB}^{slip}(Cl^-) = 0$ whereas Na^+ moves with a well-defined solvation shell. The 25 °C result of ref 25 for the effective cation solvation number can be expressed as $Z_{IB}^{slip}(Na^+) = 1/(a_o + a_1c^2 + a_2c^{5/2})$ with $a_o = 0.224 \pm 0.008$, $a_1 = 0.044 \pm 0.015$ dm^6 mol^{-2}, and $a_2 = -0.015 \pm 0.008$ dm$^{15/2}$ mol$^{-5/2}$ ($\sigma_{fit} = 0.4$). It is included as curve 4 in Figure 6. At $c = 0$ this representation yields $Z_{IB}^{slip}(Na^+,0) = 4.5 \pm 0.2$ (note that ref 25 gives the average of $Z_{IB}^{slip}(Na^+,0)$ from measurements at four temperatures). Using these data the effective solvation number of SO_4^{2-} can be calculated to be

$$Z_{IB}^{slip}(SO_4^{2-},c) = Z_{IB}^{slip}(Na_2SO_4,c) - 2Z_{IB}^{slip}(Na^+,c) \quad (24)$$

with $Z_{IB}^{slip}(SO_4^{2-},0) = 10.0 \pm 0.7$, curve 3. Note that the assumption of negligible kinetic depolarization yields the similar value of $Z_{IB}^{\xi=0}(SO_4^{2-},0) = 9.7 \pm 0.6$.

Although such comparisons must be regarded with caution since the effective solvation number deduced from DRS may include contributions from beyond the first hydration shell, $Z_{IB}^{slip}(SO_4^{2-},0)$ compares favorably with the data compiled by Ohtaki and Radnai[49] for the average coordination number, $n_-(SO_4^{2-})$, of sulfate. These data, obtained from diffraction studies and computer simulations, range from 7 to 12, with most sources giving $n_- \approx 8$. *A priori*, more appropriate is a comparison of Z_{IB} with primary solvation numbers, n_{PSO}, as defined by Bockris and Reddy.[50] Marcus gives values of 6.9, derived from the entropy of hydration, and 10.6, deduced from apparent molal isothermal compressibility data.[51] The latter agrees especially well with $Z_{IB}^{slip}(SO_4^{2-},0)$. However, the value derived from an electrostriction model ($n_{PSO} = 3.1$[52]) is considerably smaller.

A remarkable feature of $Z_{IB}^{slip}(SO_4^{2-},c)$ is the pronounced decrease at $c > 0.4$ mol dm^{-3}, which is well outside the error indicated by the standard deviations of $Z_{IB}^{slip}(Na_2SO_4,c)$ and $Z_{IB}^{slip}(Na^+,c)$. At the highest concentration, the effective solvation number has dropped to about half the value of $Z_{IB}^{slip}(SO_4^{2-},0)$. Although the formation of a SSIP is probably associated with the release of at least one water molecule, ion-pair formation alone cannot explain this observation. As argued in ref 25, this "release" of solvent molecules probably reflects the cosphere overlap of the ions at high concentration.

In ref 25 a "chemical" model for the water relaxation time of aqueous electrolytes (τ_3 in this study) was proposed. This three-state model assumes that τ_3 is a weighted average of the dwelling times of water molecules as they pass from the ground state determined by the average number of hydrogen bonds per water molecule to the activated state, where at most a single H-bond is left. *A priori*, these dwelling times should be different for water molecules in the bulk (τ_0), around cations (τ_+), and around anions (τ_-) with the weighting factors given by the relative water concentrations in these environments. This leads to

$$\tau_3^{-1}(c) = c_s/[2Z_{IB}^{slip}(Na^+)(\tau_+^{-1} - \tau_0^{-1})\,c + Z_{IB}^{slip}(SO_4^{2-})\,(\tau_-^{-1} - \tau_0^{-1})\,c + c_s\tau_0^{-1}] \quad (25)$$

If τ_0 and τ_+ are preset to $\tau_0 = \tau_3(0) = 8.26$ ps and $\tau_+ = 20$ ps, eq 25 yields a good fit to $\tau_3(c)$ at $c \leq 1$ mol dm^{-3} (the range where τ_3 was treated as an adjustable parameter; *cf.* section 2) yielding $\tau_- = 2.84 \pm 0.02$ ps ($\sigma_{fit} = 0.06$ ps). However, this result must be regarded with caution because the values obtained for τ_- and τ_+ (if also treated as an adjustable parameter) strongly depend on the concentration range used for the fit. Also, no reference data are available for τ_- from MD simulations or from other spectroscopic techniques. Similar to the situation with Z_{IB}, further investigations are necessary to build up a sufficiently large data base for τ_+ and τ_- to check the self-consistency of

the three-state model for the water relaxation time of aqueous electrolyte solutions.

5. Conclusions

Combining the present precise complex permittivity spectra determined with a vector network analyzer system covering $0.2 \leq \nu/\mathrm{GHz} \leq 20$ with waveguide interferometer data from the literature at $12 \leq \nu/\mathrm{GHz} \leq 89$, it has been possible to show that aqueous Na_2SO_4 solutions contain a considerable fraction of ion-pairs $[NaSO_4]^-_{aq}$. The association constant extrapolated from these data for $c \rightarrow 0$ is in good agreement with reliable literature values. The DRS spectra revealed two ion-pair relaxation processes that can be assigned to doubly-solvent separated (2SIP) and solvent-shared (SSIP) ion pairs. 2SIP predominates below 0.2 mol dm^{-3} but becomes negligible at high concentrations, whereas the level of SSIP remains high. Interestingly, at high ionic strength the $\beta_{NaSO_4^-}$ values determined in this investigation for aqueous Na_2SO_4 are considerably smaller than the potentiometric results obtained for dilute solutions of Na_2SO_4 in (more or less) inert background electrolytes. Some possible explanations for this are suggested.

From the solvent dispersion amplitude, the effective solvation number of SO_4^{2-} was determined as a function of the electrolyte concentration. It was found that kinetic depolarization under slip boundary conditions applies. $Z_{IB}^{slip}(SO_4^{2-},c)$ decreases significantly, at the highest concentration dropping to about half of its value at infinite dilution. The water relaxation times of the solutions can be fitted with a three-state model proposed earlier,[25] but this "chemical" model needs further investigation.

Acknowledgment. This work was funded by the Australian alumina industry and the Australian Research Council through the Australian Mineral Industries Research association Project P380B. Support by the Deutsche Forschungsgemeinschaft for R.B. is gratefully acknowledged. The authors also wish to thank one of the referees for bringing ref 10 to their attention.

References and Notes

(1) Riley, J. P., Skirrow, G., Eds. *Chemical Oceanography*, 2nd ed.; Wiley: London, 1975.

(2) Johnson, K. S.; Pytkowicz, R. M. *Ion Association and Activity Coefficients in Multicomponent Solutions*; In Activity Coefficients in Electrolyte Solutions; Pytkowicz, R. M., Ed.; Vol. 2; CRC Press: Boca Raton, FL, 1979.

(3) Pokrovski, G. S.; Schott, J.; Sergeyev, A. S. *Chem. Geol.* **1995**, *124*, 253.

(4) Pearson, T. G. *The Chemical Background of the Aluminium Industry*; Royal Institute of Chemistry: London, 1955.

(5) Holmes, H. F.; Mesmer, R. E. *J. Solution Chem.* **1986**, *15*, 495.

(6) Obšil, M.; Majer, V.; Grolier, J.-P. E.; Hefter, G. T. *J. Chem. Soc., Faraday Trans.* **1996**, *92*, 4445.

(7) Baabor, J. S.; Gilchrist, M. A.; Delgado, E. J. *J. Solution Chem.* **1998**, *27*, 67.

(8) Capewell, S.; Hefter, G. T.; May, P. M. *Talanta*, in press.

(9) Eigen, M.; Tamm, K. *Z. Elektrochem.* **1962**, *66*, 93.

(10) Gilligan, T. J.; Atkinson, G. *J. Phys. Chem.* **1980**, *84*, 208.

(11) Hester, R. E.; Plane, R. A. *Inorg. Chem.* **1964**, *3*, 769.

(12) Daly, F. P.; Brown, C. W.; Kester, D. R. *J. Phys. Chem.* **1972**, *76*, 3664.

(13) Fujita, K.; Kimura, M. *J. Raman Spectrosc.* **1981**, *11*, 108.

(14) Rudolph, W. W. *J. Chem. Soc., Faraday Trans.* **1998**, *94*, 489.

(15) Barthel, J.; Hetzenauer, H.; Buchner, R. *Ber. Bunsen-Ges. Phys. Chem.* **1992**, *96*, 1424.

(16) Pottel, R. *Ber. Bunsen-Ges. Phys. Chem.* **1965**, *69*, 363.

(17) Farber, H.; Petrucci, S. *Dielectric Spectroscopy*; In The Chemical Physics of Solvation, Part B; Dogonadze, R. R., Kálmán, E., Kornyshev, A. A., Ulstrup, J., Eds.; Elsevier: Amsterdam, 1986.

(18) Buchner, R.; Barthel, J. *Annu. Rep. Prog. Chem., Sect. C* **1994**, *91*, 71.

(19) Kaatze, U. *J. Solution Chem.* **1997**, *26*, 1049.

(20) Barthel, J.; Buchner, R.; Eberspächer, P.-N.; Münsterer, M.; Stauber, J.; Wurm, B. *J. Mol. Liq.* **1998**, *78*, 82.

(21) Barthel, J.; Hetzenauer, H.; Buchner, R. *Ber. Bunsen-Ges. Phys. Chem.* **1992**, *96*, 988.

(22) Buchner, R.; Hefter, G. T.; Barthel, J. *J. Chem. Soc., Faraday Trans.* **1994**, *90*, 2475.

(23) (a) Böttcher, C. F. J. *Theory of Electric Polarization*, 2nd ed.; Elsevier: Amsterdam, 1973; Vol. 1. (b) Böttcher, C. F. J.; Bordewijk, P. *Theory of Electric Polarization*, 2nd ed.; Elsevier: Amsterdam, 1978; Vol. 2.

(24) Buchner, R.; Barthel, J. *Ber. Bunsen-Ges. Phys. Chem.* **1997**, *101*, 1509.

(25) Buchner, R.; Hefter, G. T.; May, P. M. *J. Phys. Chem. A* **1999**, *103*, 1.

(26) (a) Sipos, P.; Bodi, I.; May, P. M.; Hefter, G. Formation of NaOH°(aq) and $NaAl(OH)^\circ_4$(aq) Ion-pairs in Concentrated Alkaline Aluminate Solutions; In *Progress in Coordination and Organometallic Chemistry*; Ondrejovicz, G.; Sirota, A. Slovak Technical Press: Bratislava, 1997. (b) Sipos, P.; Hefter, G.; May, P. M. *Aust. J. Chem.* **1998**, *51*, 445. (c) Sipos, P.; Capewell, S. G.; May, P. M.; Hefter, G.; Laurenczy, G.; Lukacs, F.; Roulet, R. *J. Chem. Soc., Dalton Trans.* 1998, 3007. (d) Radnai, T.; May, P. M.; Hefter, G.; Sipos, P. *J. Phys. Chem. A* **1998**, *102*, 7841.

(27) Barthel, J.; Buchner, R.; Münsterer, M. *ELECTROLYTE DATA COLLECTION, Part 2: Dielectric Properties of Water and Aqueous Electrolyte Solutions*; In Kreysa, G., Ed.; *Chemistry Data Series*, Vol. XII; DECHEMA: Frankfurt, 1995.

(28) Casteel, J. F.; Amis, A. S. *Chem. Eng. Data* **1972**, *17*, 55.

(29) Göttmann, O.; Kaatze, U.; Petong, P. *Meas. Sci. Technol.* **1996**, *7*, 525.

(30) Barthel, J.; Kleebauer, M.; Buchner, R. *J. Solution Chem.* **1995**, *24*, 1.

(31) Buchner, R. *Habilitationsschrift*; Regensburg, 1996.

(32) Dote, J. L.; Kivelson, D.; Schwartz, R. N. *J. Phys. Chem.* **1981**, *85*, 2169.

(33) Dote, J. L.; Kivelson, D. *J. Phys. Chem.* **1983**, *87*, 3889.

(34) Buchner, R.; Barthel, J.; Gill, B. *Phys. Chem. Chem. Phys.* **1999**, *1*, 105.

(35) Kivelson, D.; Spears, K. G. *J. Phys. Chem.* **1985**, *89*, 1999.

(36) Zamaitis, J. F., JR.; Clark, D. M.; Rafal, M.; Scrivner, N. C. *Handbook of Aqueous Electrolyte Thermodynamics, Theory and Applications*; DIPPR Publication: New York, 1986.

(37) Reardon, E. J. *J. Phys. Chem.* **1975**, *79*, 422.

(38) Fisher, F. H.; Fox, A. P. *J. Solution Chem.* **1975**, *4*, 225.

(39) Barthel, J.; Krienke, H.; Kunz, W. *Physical Chemistry of Electrolyte Solutions*; Steinkopff/Springer: Darmstadt/New York, 1998.

(40) Luts, P.; Vanhees, L. J. C.; Yperman, J. H. E.; Mullens, J. M. A.; Van Poucke, L. C. *J. Solution Chem.* **1992**, *21*, 375.

(41) Sapiezko, R. S.; Patel, R. C.; Matijevic, E. *J. Phys. Chem.* **1977**, *81*, 1061.

(42) Santos, M. M.; Guedes de Carvalho, J. R. F.; Guedes de Carvalho, R. A. *J. Solution Chem.* **1975**, *4*, 25.

(43) Buchner, R.; Barthel, J. *J. Mol. Liq.* **1995**, *63*, 55.

(44) Padova, J. *J. Chem. Phys.* **1963**, *38*, 2635.

(45) Korosi, A.; Fabuss, B. M. *J. Chem. Eng. Data* **1968**, *13*, 548.

(46) Singh, D.; Singh, N. P.; Bahadur, L. *Indian J. Chem.* **1975**, *13*, 1177.

(47) (a) Hubbard, J. B.; Onsager, L. *J. Chem. Phys.* **1977**, *67*, 4850. (b) Hubbard, J. B. *J. Chem. Phys.* **1978**, *68*, 1649.

(48) Hubbard, J. B.; Colonomos, P.; Wolynes, P. G. *J. Chem. Phys.* **1979**, *71*, 2652.

(49) Ohtaki, H.; Radnai, T. *Chem. Rev.* **1993**, *93*, 1157.

(50) Bockris, J. O'M.; Reddy, A. K. N. *Modern Electrochemistry*, 3rd ed.; Plenum: New York, 1970; Vol. 1.

(51) Marcus, Y. *Ion Solvation*; Wiley: Chichester, 1985.

(52) Marcus, Y. *Ion Properties*; Dekker: New York, 1997.